

Effect of k_z variation of $d_{a^2-b^2}$ -wave order parameter on c -axis tunneling spectroscopy

P. Pairor *

School of Physics, Institute of Science, Suranaree University of Technology, 111 University Avenue, Nakhon Ratchasima 30000, Thailand

Received 12 May 2006; received in revised form 22 August 2006; accepted 22 August 2006

Available online 9 October 2006

Abstract

The effect of k_z variation of the superconducting $d_{a^2-b^2}$ -wave order parameter on c -axis tunneling spectra of metal–superconductor junctions is theoretically investigated. In the high transmission limit, the variation does not cause obvious changes in the shape of the conductance spectrum, while in the tunneling limit the effect is more apparent. The coherence peak of the conductance spectrum gets wider as the variation of the order parameter is larger. The effect of the variation can be seen more clearly in the spectrum of the derivative of the conductance in both limits.

© 2006 Elsevier B.V. All rights reserved.

PACS: 74.20.-z; 74.25.Jb

Keywords: d-wave superconductors; Tunneling spectroscopy; c -axis variation

1. Introduction

Features in metal–superconductor tunneling conductance spectra are caused by different characteristics of superconducting order parameter. For instance, a coherence peak in the tunneling spectra is a signature of a large number of states at the energy gap. It is well known that the peak position provides accurate measurement for the magnitude of the superconducting gap [1–3]. Tunneling spectroscopy is also a valuable tool for obtaining the gap symmetry of an unconventional superconductor (see for example Refs. [4–13]). By varying the tunneling junction orientation, for example in the case of d-wave superconductor, with respect to the crystal axes, the observation of zero-bias conductance peak can be used to locate sign changes in the gap function and consequently determine its symmetry [4–9]. There have been many tunneling experiments that revealed zero-bias

conductance peaks in the tunneling spectra of copper-oxide based superconductors (for a review see [14]). The existence of this peak in part has provided supporting evidence for $d_{a^2-b^2}$ -wave symmetry of the order parameter in these materials.

In this article, the impact on the tunneling spectrum of the pairing interaction between layers of adjacent unit cells will be discussed. This interaction, which is different from that between the layers within the unit cell (see for example [15–21]), reveals itself as k_z variation of the order parameter [22,23]: $\Delta(\phi_s, k_z) = [\Delta_0 + \Delta_1 \cos(k_z a_c)] \cos 2\phi_s$. Δ_0 and Δ_1 are the intralayer and interlayer pairing order parameter respectively. ϕ_s is the direction with respect to the a axis of the superconductor. k_z is the component along the c axis of the wave vector. a_c is the lattice constant along the c axis.

This article is organized as follows. In the next section, a brief explanation of the model and method used to calculate the current across the junction will be given. The conductance spectra of c -axis junctions in both limits will be shown and discussed in Section 3. Section 4 is the conclusion of this article.

* Fax: +66 44224185.

E-mail address: pairor@sut.ac.th

2. Model and method

The metal–superconductor junction is modeled, as depicted in Fig. 1, as an infinite system, the left half of which is a metal and the right half of which is a $d_{a^2-b^2}$ -wave superconductor. The interface normal is set to be parallel to the c axis of the $d_{a^2-b^2}$ superconductor. The insulating barrier is represented by a delta function potential of strength H , and the order parameter is taken to be [22,23]

$$\Delta_k \equiv \Delta(\phi_s, k_z) = [\Delta_0 + \Delta_1 \cos(k_z a_c)] \cos 2\phi_s, \quad (1)$$

where Δ_0 and Δ_1 are the intralayer and interlayer pairing order parameter respectively, ϕ_s is the direction with respect to the a axis of the superconductor, k_z is the component along the c axis of the wave vector, and a_c is the lattice constant along the c axis. In this article, the magnitude of the maximum gap $\Delta_{\max} = \Delta_0 + \Delta_1$ is taken to be of order a tenth of the Fermi energy of the superconductor.

To describe the excitations of the system, the following Bogoliubov-de Gennes equations with a parabolic dispersion are used

$$\begin{bmatrix} \widehat{O}_p + H\delta(z) - \mu & \Delta_k \Theta(z) \\ \Delta_k^* \Theta(z) & -(\widehat{O}_p + H\delta(z) - \mu) \end{bmatrix} U(\vec{r}) = EU(\vec{r}), \quad (2)$$

where μ is the chemical potential, $\Theta(x)$ is the Heaviside step function, and

$$\widehat{O}_p = -\frac{\hbar^2}{2m_{ab}} \left(\frac{\partial^2}{\partial x^2} + \frac{\partial^2}{\partial y^2} \right) - \frac{\hbar^2}{2m_c} \frac{\partial^2}{\partial z^2}, \quad (3)$$

where

$$m_{ab} = \begin{cases} m, & z < 0, \\ m_{ab}^s, & z > 0 \end{cases} \quad (4)$$

and

$$m_z = \begin{cases} m, & z < 0, \\ m_c^s, & z > 0, \end{cases} \quad (5)$$

where m is the effective mass of an excitation in the metal and m_{ab}^s, m_c^s are the ab -plane and the c -axis effective masses of a superconducting quasiparticle respectively. Note that although this approximate parabolic dispersion is not accu-

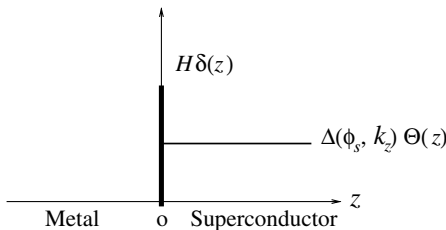


Fig. 1. The metal–superconductor junction is modeled as an infinite system. The metal and the superconductor occupy the $z < 0$ region and the $z > 0$ region respectively. The delta function of height H represents the insulating layer. The gap function $\Delta(\phi_s, k_z)$ is as described in the text.

rate for the anisotropic dispersion of the copper-oxide based superconductors, it is enough to capture essential consequences of the k_z variation of the order parameter. One can improve the model by using a more accurate tight-binding dispersion.

The two-component wave function $U(\vec{r})$ is

$$U(\vec{r}) = \begin{cases} U_M(\vec{r}), & z < 0, \\ U_S(\vec{r}), & z > 0, \end{cases} \quad (6)$$

where the subscripts M and S represent the metal and superconducting sides respectively.

Due to the translational symmetry along the plane of junction interface, the two wave functions can be written as

$$U_M(\vec{r}) = U_M(z) e^{i(k_x x + k_y y)}, \quad (7)$$

$$U_S(\vec{r}) = U_S(z) e^{i(k_x x + k_y y)}, \quad (8)$$

where $U_M(z) = U_{M0} e^{iq_z z}$ and $U_S(z) = U_{S0} e^{ik_z z}$. The matching conditions for the wave functions at the interface are

$$U_M(z=0) = U_S(z=0) \equiv U_0, \quad (9)$$

$$ZU_0 = \frac{1 + m/m_c^s}{4k_F} \left(\left. \frac{\partial U_S}{\partial z} \right|_{0^+} - \left. \frac{\partial U_M}{\partial z} \right|_{0^-} \right), \quad (10)$$

where $Z = mH/(\hbar^2 k_F)$ and k_F is the magnitude of the Fermi wave vector of the superconductor.

The bulk excitation energies for the normal metal are

$$E_q = \frac{\hbar^2}{2m} (q_z^2 + k_x^2 + k_y^2) - \mu \equiv \pm \xi_q, \quad (11)$$

where the plus and minus signs are for electron and hole excitations respectively. For the superconductor,

$$E_k = \sqrt{\xi_k^2 + |\Delta_k|^2}, \quad (12)$$

where

$$\xi_k = \pm \left(\frac{\hbar^2}{2m_{ab}^s} (k_x^2 + k_y^2) + \frac{\hbar^2}{2m_c^s} k_z^2 - \mu \right). \quad (13)$$

The amplitude of an excitation, U_{N0} , in the normal metal is $\begin{pmatrix} 1 \\ 0 \end{pmatrix}$ for an electron and is $\begin{pmatrix} 0 \\ 1 \end{pmatrix}$ for a hole, whereas the amplitude of an excitation in the superconductor is

$$U_{S0} = \frac{1}{\sqrt{|E + \xi_k|^2 + |\Delta_k|^2}} \begin{pmatrix} E + \xi_k \\ \Delta_k \end{pmatrix} \equiv \begin{pmatrix} u_k \\ v_k \end{pmatrix}. \quad (14)$$

The wave function of each side is a linear combination of all the appropriate excitations of the same energy and the momentum that has the same component perpendicular to the interface normal. That is,

$$U_M(z) = \begin{pmatrix} 1 \\ 0 \end{pmatrix} e^{iq^+ z} + a \begin{pmatrix} 0 \\ 1 \end{pmatrix} e^{iq^- z} + b \begin{pmatrix} 1 \\ 0 \end{pmatrix} e^{-iq^+ z}, \quad (15)$$

$$U_S(z) = c \begin{pmatrix} u_{k^+} \\ v_{k^+} \end{pmatrix} e^{ik^+ z} + d \begin{pmatrix} u_{-k^-} \\ v_{-k^-} \end{pmatrix} e^{-ik^- z}, \quad (16)$$

where

$$q^\pm = \sqrt{\frac{2m}{\hbar^2}(\mu \pm E) - k_x^2 - k_y^2},$$

$$k^\pm = \sqrt{\frac{2m}{\hbar^2}\left(\mu \pm \sqrt{E^2 - \Delta_k^2}\right) - k_x^2 - k_y^2}$$

are the parallel-to-the-interface-normal components of the normal and superconducting wave vectors respectively, and a, b, c, d are the Andreev reflection, the normal reflection, the same-branched transmission, and the cross-branched transmission amplitudes respectively. These amplitudes can be obtained from the matching conditions in Eqs. (9) and (10). It should be mentioned that in all the calculations related to the transmission and reflection probabilities in this work, all the terms of the same order or smaller than (Δ/E_F) , which is taken to be 0.1 in this article, are ignored. The effect of terms of order (Δ/E_F) was discussed in Ref. [24].

By following the formalism in Ref. [25], one can obtain the expression for the current across the junction as a function of applied voltage as

$$I_{MS}(V) = \frac{e\Omega}{8\pi^3} \int d^3q (1 + A(q) - B(q)) v_z \times [f(E_q - eV) - f(E)], \quad (17)$$

where Ω is the volume, v_z is the component parallel to the interface normal of the group velocity of the incoming electron, $f(E)$ is the Fermi–Dirac distribution function, and $A = |a|^2 q^- / q^+$, $B = |b|^2$ are the probabilities of Andreev

and normal reflections, respectively. The conductance can thus be obtained from

$$G(V) = \frac{dI_{MS}}{dV}. \quad (18)$$

In all cases considered in this article, the ab plane effective mass of a superconducting quasiparticle is taken to be equal to the effective mass of an excitation in the metal. The c -axis effective mass of a superconducting quasiparticle is taken to be 100 times that of the ab plane effective mass to account for the anisotropy between the ab plane and the c axis, which is at least of the order 100 [26] in most copper-oxide based superconductors.

3. Results

The normalized conductance spectra and their derivatives in different limits at zero temperature are shown in Figs. 2–4. Note that the normalized conductance is defined as the conductance divided by its value at infinite applied voltage, and the maximum gap is defined as $\Delta_{\max} = \Delta_0 + \Delta_1$. In the Andreev limit (Fig. 2), the conductance spectra show the inverted-gap structure for all values of Δ_1 . At first glance, the effect of non-zero values of Δ_1 is not very obvious on the overall shape of the conductance spectra. The peak of the inverted-gap structure at zero voltage is unaffected by the variation of the order parameter. Taking a closer look, one can then see that the non-zero values of Δ_1 result in a kink, or the abrupt change in the

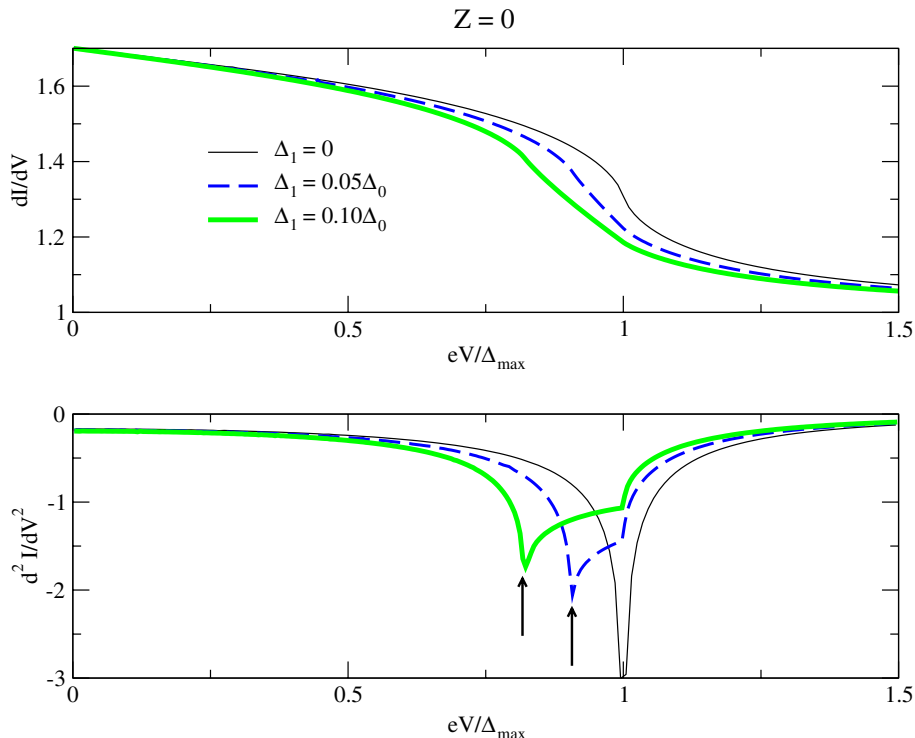


Fig. 2. On the top panel, three normalized conductance curves with different values of Δ_1 are shown. The value of Z is set to 0 to reflect the Andreev limit. The plots of the derivatives of the conductance spectra are shown in the lower panel, where the arrows indicate the features occurring at $\Delta_0 - \Delta_1$.

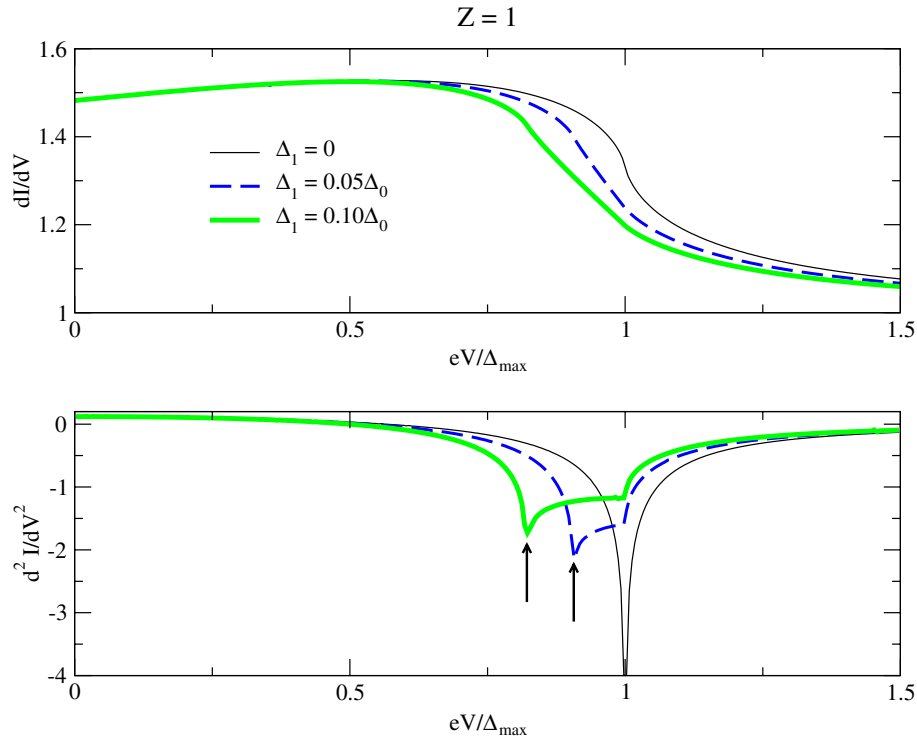


Fig. 3. On the top panel, three normalized conductance spectra with different values of Δ_1 are shown. The value of Z is set to 1. The plots of the derivatives of the conductance spectra are shown in the lower panel, where the arrows indicate the features occurring at $\Delta_0 - \Delta_1$.

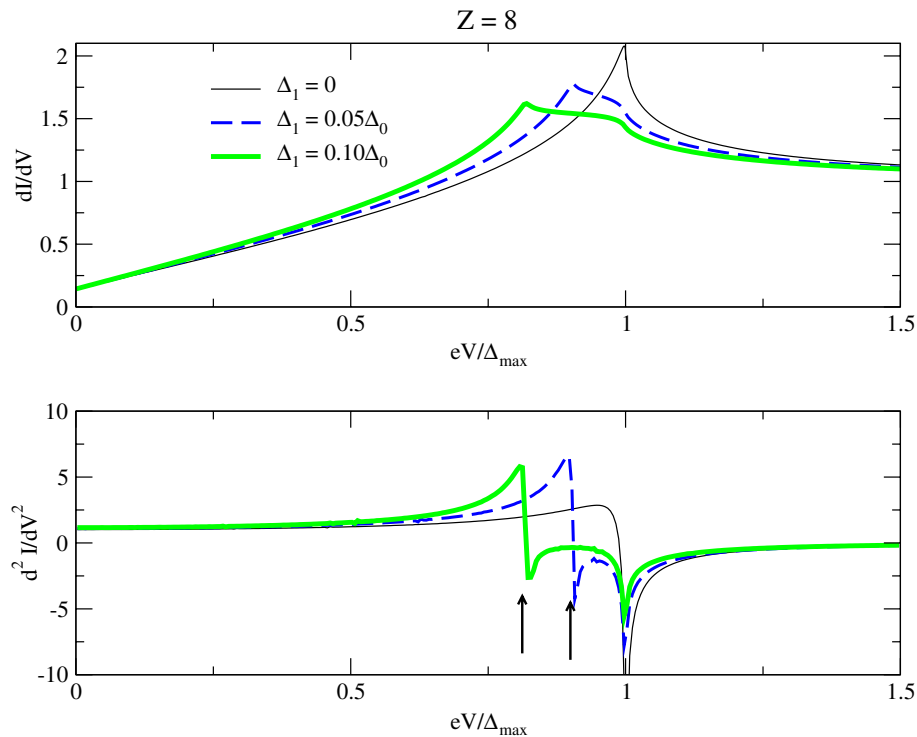


Fig. 4. On the top panel, three normalized conductance curves with different values of Δ_1 are shown. The value of Z is set to 8. The plots of the derivatives of the conductance curves are shown in the lower panel, where the arrows indicate the features occurring at $\Delta_0 - \Delta_1$.

slope of the conductance, at $\Delta_0 - \Delta_1$. This change can be seen more easily as a sharp dip at $\Delta_0 - \Delta_1$ in the plot of the derivative of the conductance spectrum.

The conductance spectra in the intermediate limit (Fig. 3) are similar to those in the Andreev limit. The overall shape of the conductance spectrum is very little affected

by the c -axis variation of the order parameter. The effect is more obvious in the plots of derivatives of the conductance spectra, which show similar features to those in the Andreev limit.

Unlike in the Andreev limit, the effect of the variation can be clearly seen in the conductance spectra in the tunneling limit. The coherence peak around the maximum gap becomes wider as Δ_1 gets bigger. The peak-like edge moves inwards and away from Δ_{\max} , as Δ_1 is increased. More specifically, the position of this edge occurs at $\Delta_0 - \Delta_1$. At Δ_{\max} , the feature occurring instead is an inflection point. The effect is also obvious in the plot of the derivative of the conductance spectrum. At $\Delta_0 - \Delta_1$, the derivative of the conductance spectrum changes sign from positive to negative and at the maximum gap a very sharp dip occurs.

4. Conclusion

This article is a theoretical investigation of the consequence of the c -axis interlayer pairing interaction in c -axis tunneling spectroscopy. Such interaction results in a variation in the gap function along k_z . This variation more obviously affects the conductance spectrum in the tunneling limit than in the Andreev limit. Particularly, the variation causes the widening of coherence peak in the tunneling limit, whereas in the Andreev limit it causes a change in slope around the maximum gap. The width of the coherence peak in the conductance spectrum in the tunneling limit and the distance in energy between the two distinguished features in the derivative of the conductance spectrum in both limits are proportional to the interlayer pairing order parameter, Δ_1 .

The k_z variation of the order parameter is expected to affect the in-plane tunneling spectra in a similar fashion as well. As shown in Ref. [27], in the tunneling limit the coherence peak becomes wider as Δ_1 gets bigger and its width is also proportional to Δ_1 .

Acknowledgement

The author would like to thank Thailand Toray Science Foundation (TTSF) for the financial support.

References

- [1] E.L. Wolf, Principles of Electron Tunneling Spectroscopy, Oxford University Press, New York, 1989.
- [2] W.L. McMillan, J.M. Rowell, in: R.D. Parks (Ed.), Superconductivity, vol. 1, Marcel-Dekker, New York, 1969, p. 561.
- [3] M. Tinkham, Introduction to Superconductivity, McGraw-Hill, New York, 1996.
- [4] C.-R. Hu, Phys. Rev. Lett. 72 (1994) 1526.
- [5] J. Yang, C.-R. Hu, Phys. Rev. B 50 (1994) 16766.
- [6] S. Kashiwaya, Y. Tanaka, M. Koyanagi, K. Kajimura, Phys. Rev. B 53 (1996) 2667.
- [7] Y. Tanaka, S. Kashiwaya, Phys. Rev. Lett. 74 (1995) 3451.
- [8] C.-R. Hu, Phys. Rev. B 57 (1998) 1266.
- [9] P. Pairor, M.B. Walker, Phys. Rev. B 65 (2002) 064507.
- [10] N. Stefanakis, Physica C 369 (2002) 304.
- [11] P. Pairor, M.F. Smith, J. Phys.: Condens. Matter 15 (2003) 4457.
- [12] Y. Tanuma, Y. Tanaka, K. Kuroki, S. Kashiwaya, Physica C 437438 (2006) 319.
- [13] Y. Tanuma, Y. Tanaka, S. Kashiwaya, Physica C 412414 (2004) 319.
- [14] Guy Deutscher, Rev. Mod. Phys. 77 (2005) 109.
- [15] B.W. Hoogenboom, C. Berthod, M. Peter, Ø. Fischer, A.A. Kordyuk, Phys. Rev. B 67 (2003) 224502.
- [16] P.K. Pathak, Ajay, Physica C 423 (2005) 137.
- [17] A. Singh, P.K. Pathak, Ajay, R. Kishore, Physica C 415 (2004) 145.
- [18] Y.H. Su, J. Chang, H.T. Lu, H.G. Luo, T. Xiang, Phys. Rev. B 68 (2003) 212501.
- [19] W. Kim, J.P. Carbotte, Phys. Rev. B 63 (2001) 054526.
- [20] W.-C. Wu, Phys. Rev. B 65 (2002) 052508.
- [21] S.E. Barnes, S. Maekawa, Phys. Rev. B 67 (2003) 224513.
- [22] A.K. Rajagopal, S.S. Jha, Phys. Rev. B 54 (1996) 4331.
- [23] S.S. Jha, A.K. Rajagopal, Phys. Rev. B 55 (1997) 15248.
- [24] A. Golubov, F. Tafuri, Phys. Rev. B 62 (2000) 15200.
- [25] G.E. Blonder, M. Tinkham, K. Klapwijk, Phys. Rev. B 25 (1987) 4515.
- [26] C.P. Poole, H.A. Farach, R.J. Creswick, Superconductivity, Academic Press, New York, 1995, p. 154.
- [27] P. Pairor, Phys. Rev. B 72 (2005) 174519.